This is the Pre-Published Version.
This is the accepted version of the publication Zeng, J., Cao, H., & Hu, H. (2019). Finite element simulation of an auxetic plied yarn structure. Textile Research Journal, 89(16), 3394-3400. Copyright © The Author(s) 2018. DOI: 10.1177/0040517518813659.

Finite Element Simulation of Auxetic Plied Yarn Structure

Jifang Zeng[1], Haijian Cao[2] and Hong Hu[1]

[1] Institute of Textile and Clothing, Hong Kong Polytechnic University, Hung Hom, Kowloon, Hong Kong, China

[2] School of Textile and Clothing, Nantong University, Nantong, Jiangsu 226019, China

Email: hu.hong@polyu.edu.hk

Abstract: The auxetic plied yarn is a novel type of yarn structure formed with two types of component yarns having different moduli. Although the effect of structural parameters on its negative Poisson's ratio behavior has been investigated by both experimental and geometrical analyses, the influence of material properties including yarn tensile modulus and friction has not been studied yet. In this work, these two factors are further investigated via finite element simulation. The finite element model is first created by using commercial software ANSYS 15.0. Then, the simulation results are compared with the experimental and analytical data. Finally, the effects of the tilt angle of stiff yarn, yarn friction and tensile modulus are discussed. It is expected that the outcomes of this work would be useful to guide the design and fabrication of this type of auxetic yarn structure.

Keywords: Finite element model, auxetic plied yarn, negative Poisson's ratio, deformation behavior

1. Introduction

The auxetic materials[1], which are contrary to most of the conventional materials, have a negative Poisson's ratio. Due to their particular internal structure, they become thicker when stretched or vice versa.

The auxetic materials rang from the nanoscale to the macroscale and involve different types of materials such as metals[2], ceramics[3], polymers[4, 5], textiles[6-8], composites[9], etc. Owing to their unusual deformation behavior, the auxetic materials can achieve a number of significant superb mechanical properties, such as enhanced indentation resistance, improved fracture strength, high vibration damping behavior and formation of synaclastic curvature under out-of-plane bending. In the past three decades, lots of efforts have been made on their fabrication[6, 10-12], characterization[13-16] and applications [1, 17-19]. The research works on auxetic materials have been reviewed by Lim[20], Alderson [10], Liu [5], Ma [8], Mir [21] and Lakes[22].

This study focuses on the finite element simulation of an auxetic plied yarn structure. Based on our knowledge, the research on the auxetic plied yarn is still very limited. Up to now, most of publications are related to the helical yarn structure [23-30]. The helical yarn structure was firstly proposed by Evans in 2008. It is formed with two yarn elements, a core yarn and a wrap yarn. While the core yarn with higher elasticity is kept straight at the initial state, the wrap yarn with higher tensile modulus is helically wound on it. Due to the significant difference in modulus, the core yarn becomes a helical form under the uniaxial stretching strain. When the diameter of the core yarn is much larger than that of the wrap yarn, the effective diameter of the helical yarn will get increased with increasing the uniaxial stretching strain, resulting in an achievement of negative Poisson's ratio. The experimental and numerical studies have shown that the initial helical angle [23] and diameter of the wrap yarn[25, 26], the diameter and tensile modulus of the core yarn are important factors to affect the negative Poisson's ratio behavior of the helical yarn structure. Particularly, the influence of the helical angle of the wrap yarn is much more significant than others[23], and the maximum negative Poisson's ratio effect of the helical yarn structure can be increased with decreasing the helical angle of the wrap yarn. According to McAfee J and Faisal NH[23], the maximum negative Poisson's ratio can reach -12.04 when the helical angle is decreased to 7 degree. It was also found that the Poisson's ratio of the wrap yarn has a slight influence on the negative Poisson's ratio behavior of the helical auxetic yarn. It should be noted that although the fabrication of the auxetic helical yarn is simple, the helical angle of the wrap yarn can vary throughout the whole helical yarn as the slippage of the wrap yarn easily occurs on the surface of the core yarn. Especially, this uneven state can take place after repeated extension, which severely impedes the application of the helical yarn. To solve this problem, an appropriate layer of sheath was proposed to enclose the helical yarn[24]. This not only facilitates the fabrication, but also enlarges the application of the helical yarn.

The auxetic plied yarn is another type of auxetic yarn structure in which two stiff yarns with higher modulus and two soft yarns with lower modulus are alternatively arranged and twisted together. Ge et al.[12] first conducted an experimental investigation on this type of yarn structure and found that its negative Poisson's ratio effect first increased and then decreased with the applied tensile strain. A later experimental study by Ng et al. further confirmed this variation trend [31]. In order to theoretically predict the deformation behavior of the auxetic plied yarn structure, Ge et al. also performed a geometrical analysis[12]. Although their analysis could provide the precise prediction of Poisson's ratio at higher tensile strain, the predicted trend at the initial tensile strain is opposite to that of the experiment. To reduce this disagreement, an improved geometrical model by introducing a tilted angle of the stiff yarn at the initial state was proposed by Zeng et al.[32] The new model could well predict the variation trend of the deformation behavior of the auxetic plied yarn structure. Although the effects of various structural parameters including the helical angle, the diameter and the Poisson's ratio of the component yarns have been systematically investigated in these geometrical analyses, the influence of the component yarn's material properties including tensile modulus and friction effect could not be included in the geometrical analysis. In this work, these two factors will be further investigated by the finite element simulation by using the commercial software ANSYS 15.0.

2. Geometry of auxetic plied yarn structure

An ideal auxetic plied yarn structure is schematically shown in Fig.1a. It is constructed by two types of component yarns which are helically twisted together. The one is called soft yarn, because its tensile modulus is smaller than the other one. Hence, the other one is named as stiff yarn. As shown in Fig. 1b, each stiff yarn closely contacts two neighboring soft yarns at the initial state. Fig. 1c shows one turn of the yarn structure. The parameters which were used to characterize the geometry of the auxetic yarn structure in [32] are also shown in Fig.1b and 1c, respectively. They are diameter D and helical angle θ_D of the soft yarn, diameter d and helical angle θ_d of the stiff yarn, effective diameter H and length per turn L of the plied yarn, coordinate locations y_D and x_d of the soft yarn and stiff yarn, respectively. In fact, these structural parameters are not completely independent. In this work, diameters D and d of the soft and stiff yarns, helical angle θ_D of the soft yarn and length L of the plied yarn in one turn are selected as independent structural parameters.

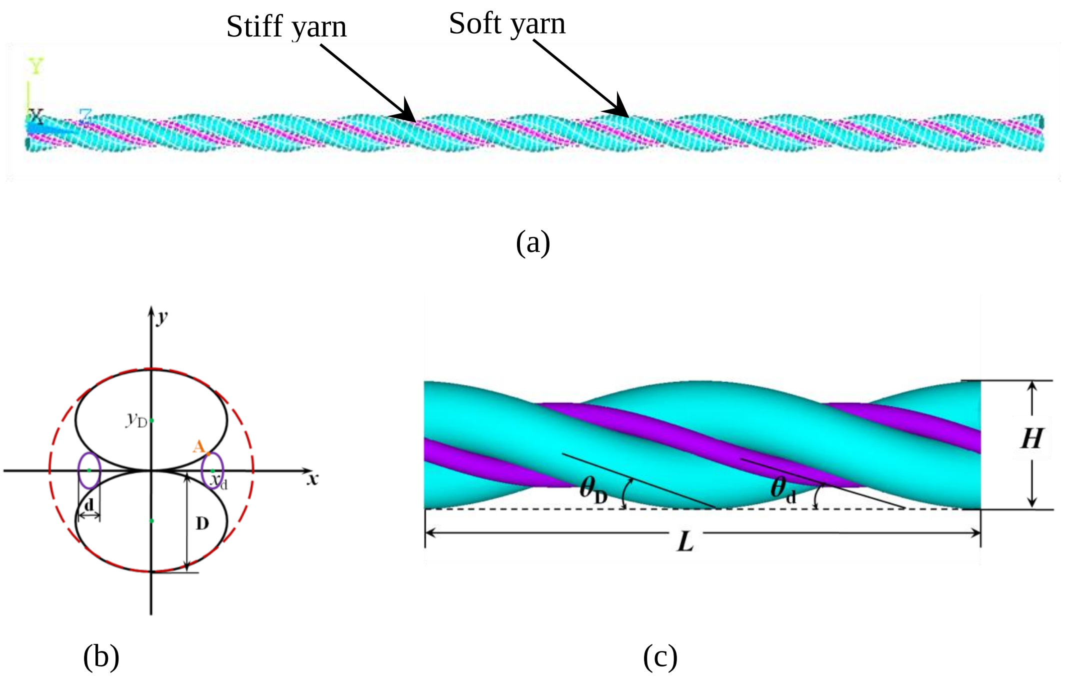

Figure 1. Schematic illustration of an ideal auxetic plied yarn structure: (**a**) 3D view; (**b**) cross sectional view; (**c**) one turn of the yarn structure. Note: the geometrical parameters shown in (**b**) and (**c**) are the same as shown in[32].

3. Creation of finite element model

Before the creation of the finite element model, the following assumptions are firstly made to facilitate the simulation according to the experimental observations.

1) The cross sections of both the soft and stiff yarns are in perfect circle form.

2) The soft and stiff yarns are isotropic materials.

3) The two soft yarns closely contact each other at the initial state.

4) The stretching process of the auxetic plied yarn structure under uniaxial extension are divided into two stages by critical strain ε_c at which the two stiff yarns just get contacted to each other at the center of the auxetic plied yarn.

5) The twist of the auxetic plied yarn structure is uniform and one turn of the yarn can represent the deformation behavior of the whole plied yarn structure. Therefore, the finite element model is only created for one turn of the yarn structure to save the time of the calculation.

6) Each stiff yarn has contact with only a single soft yarn at the initial state due to de-twisting trend of the yarn in a real auxetic plied yarn structure and its initial position is determined by a tilt angle *T* as shown in Fig. 2. The structure shown in Fig. 1b is only an ideal case when *T* = 0.

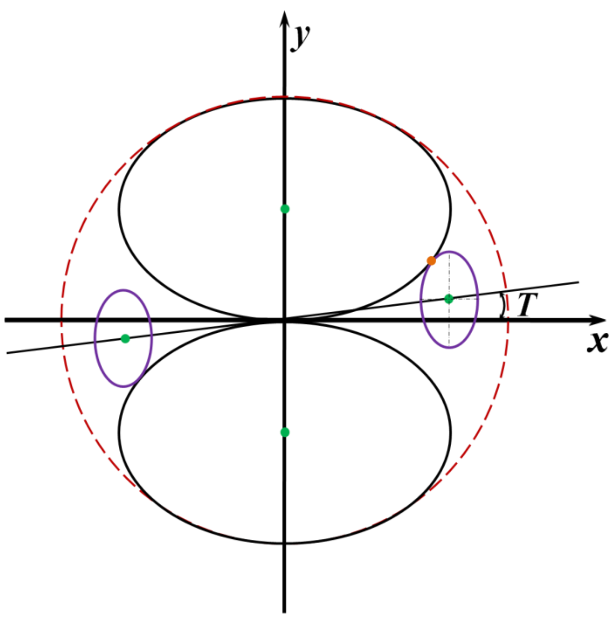

Figure 2. The cross section of a real auxetic plied yarn at the initial state

Based on these assumptions, the finite element models were created using commercial software ANSYS 15.0. The geometrical parameters listed in Table 1[31] were first used to create the control model without the consideration of friction between the stiff yarn and soft yarn. The material properties of the component yarns used are listed in Table 2. The three-dimensional (3D) structural element SOLID185 was used to create both the soft and stiff yarns with their own mechanical properties. A 3D contact pair is composed by TARGE170 and CONTA173 to represent contact and sliding between the soft and stiff yarns. As shown in Fig. 3, the finite element model for one turn of the auxetic plied yarn was created using the bottom-up direct generation method. A helical path on the surface of one soft yarn was firstly created with given helical angle θ_{D0} and length per turn L_0 at the initial state as shown in Fig. 3a. Then, one soft yarn was created with given diameter D_0 at the initial state via a cylindrical coordinate system as shown in Fig. 3b. Next, the other soft yarn was created by generation operation using the first soft yarn. In the same way, two stiff yarns were created with given diameter d_0 and tilt angle of the stiff yarn T after the working plane's X-Y coordinate system had been rotated 45^{o}. Until here, the geometrical model of one turn of the plied yarn structure was created as displayed in Fig. 3c. After the geometric model had been created, the cross sections of yarns were defined as the source mesh to sweep the yarns to create the finite element model as shown in Fig. 3d. As shown in Fig. 3e, in total there are five contact pairs: one is for the contact between two stiff yarns and the rest four contact pairs for the contacts between the soft yarns and their adjacent stiff yarns.

Table 1. The geometrical parameters[31] at the initial state used for the theoretical calculation and finite

element simulation

Auxetic plied yarn	**Stiff yarn**	**Soft yarn**	
Length per turn L_0 (mm)	Diameter d_0 (mm)	Diameter D_0 (mm)	Helical angle θ_{D0} (°)
19.60	0.77	2.18	19.26

Note: the tilt angle of the stiff yarn T is 2.91° and subscript 0 is the indication of the initial state.

As for the boundary condition, the symmetry boundary condition was applied to one end of the plied yarn structure and the displacement load was imposed to the other end of the plied yarn. Then, the large-deflection effects were turned on and the updated Newton-Raphson method was used to accelerate the solution convergence.

Table 2. The mechanical properties of the component yarns used for finite element simulation

Soft yarn			**Stiff yarn**		
E (MPa)	υ	μ	E (MPa)	υ	μ
13	0.15	0	1300	0.15	0

Note: E is the tensile modulus, υ is the Poisson's ratio and μ is the friction coefficient.

(a)

(b)

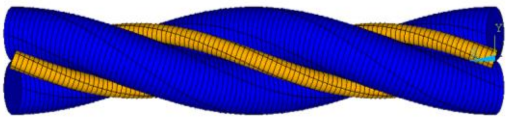

(c)

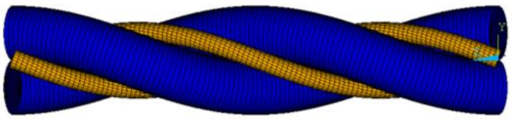

(d)

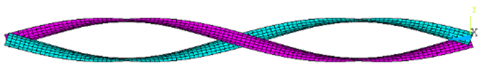

Stiff yarn(cyan) to stiff yarn(pink)

Soft yarn(cyan) to stiff yarn(pink)

(e)

Figure 3. The creation process of the finite element model: (**a**) one helical path on the surface of one soft yarn; (**b**) one soft yarn; (**c**) the plied yarn geometrical model; (**d**) the finite element model; (**e**) the contact pairs.

4. Results and discussion

4.1 Comparison with experimental and geometrical analyses

As shown in Fig. 4, the final element simulation results obtained from the finite element model are compared with the experimental results from Ng et al. work [31] and the geometrical analysis from the tilted angle model [32] using the same parameters values listed in Table 1 and Table 2. Obviously, the variation trend of Poisson's ratio with the applied tensile strain from the finite element simulation is similar to the experimental [31] and theoretical one[32]. Especially, the values of Poisson's ratio obtained from the simulation and the geometrical analysis are nearly the same when the applied tensile strain is larger than the critical strain. However, as the friction effect between the soft and stiff yarns was not taken into the consideration, the negative Poisson's ratio effect is overestimated by both the finite element simulation and the geometrical analysis compared to the experimental data. In addition, the maximum negative Poisson's ratio effect by the finite element simulation is higher than that of the geometrical analysis. This difference could be explained by faster reaching of the stiff yarns from their initial position to the center of the plied yarn structure at a lower tensile strain due to ignorance of friction.

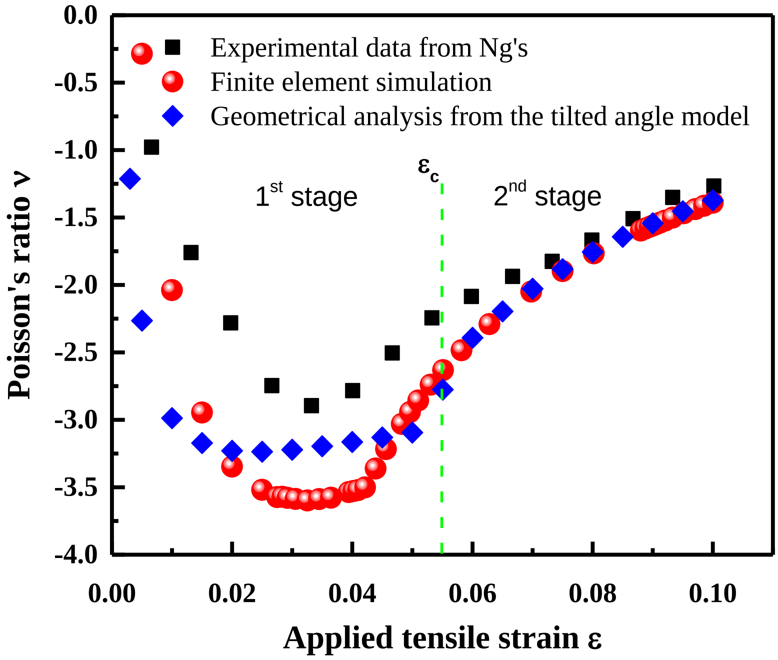

Figure 4. A comparison of the Poisson's ratio as a function of applied tension strain among the experiment [31], the finite element simulation and the geometrical analysis based on the tilted angle model [32].

4.2 The effect of tilt angle of the stiff yarn

To systematically study the effect of the tilted angle of the stiff yarn on the negative Poisson's ratio behavior of the auxetic plied yarn structure, the tilted angle of the stiff yarn was varied from 0 to 2.9°. This range of the tilted angle was selected according to the experimental observation. The simulation results together with the experimental data are shown in Fig. 5. Here, the finite element model with a tilt angle of zero ($T = 0$) is considered as an ideal case of the auxetic yarn structure and this case has been geometrically investigated by Ge et al.[12] The variation trend of Poisson's ratio with applied tensile strain obtained by the finite element simulation is the same as calculated by Ge's analysis [12] for this ideal case. Fig. 5 clearly shows that the tilt angle of the stiff yarn has a significant influence on the deformation behavior of the auxetic plied yarn structure at the first stage of the extension process and the change of the value of T from 0 to a positive value can lead to the change of the variation trends of Poisson's ratio from a monotonic mode to a parabolic form. In addition, a difference is found between the finite element simulation and the geometrical analysis when the value of T is not zero. According to the geometrical analysis [32], the influence of the tilt angle with different positive values is not evident. This difference could be explained by the fact that the yarn material properties can be included in the finite element simulation, but cannot be included in the geometrical analysis.

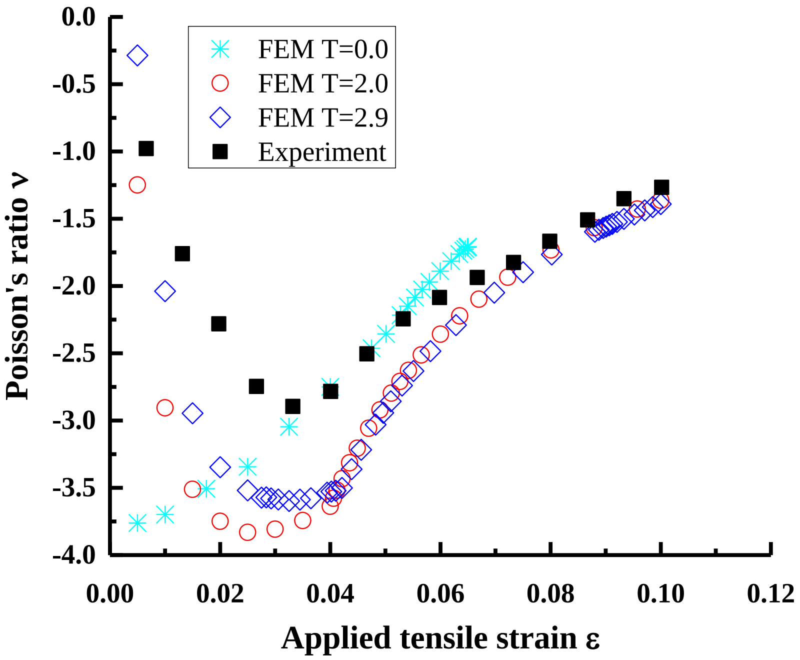

Figure 5. The effect of tilt angle (T) on the negative Poisson's ratio behavior of the plied yarn structure. For comparison, the experimental results are also presented.

4.3 The effect of friction

To save the time of the calculation, the effect of friction between the stiff yarn and soft yarn was not taken into the consideration in the above simulations. In fact, the friction between the yarns is an important factor which can have an obvious influence on the negative Poisson's ratio behavior of the plied yarn structure. To analyze the effect of friction, the finite element model when $T = 0$ was used to simulate the negative Poison's ratio behavior of the plied yarn structure. The simulation results with different values of friction coefficient μ are shown in Fig. 6. It can be seen that the negative Poisson's ratio effect is reduced when the friction coefficient is increased from 0 to 0.01. Luckily, the negative Poisson's ratio effect is found the same for μ=0.01 and μ=0.05. In fact, the friction coefficient between the yarns could be between 0 and 1. Hence, to obtain better negative Poisson's ratio effect, the friction coefficient should be minimized as possible.

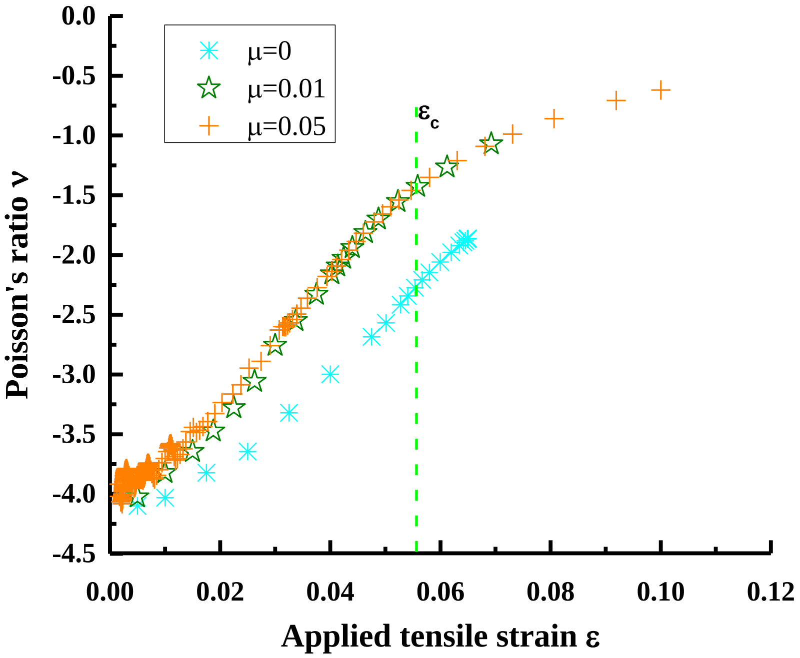

Figure 6. The effect of friction on the negative Poisson's ratio behavior of the plied yarn structure.

4.4 The effect of tensile modululi of component yarns

In order to study the effect of the tensile moduli of both the soft yarn and stiff yarn on the negative Poisson's ratio behavior of the auxetic plied yarn structure, a moduli ratio E^* defined by Eq.1 was firstly introduced.

$$E^* = \frac{E_{stiff}}{E_{soft}} \tag{1}$$

Where E_{stiff} and E_{soft} are the tensile moduli of the stiff yarn and soft yarn, respectively. To analyze the effect of E^*, the finite element model when $T = 0$ was used to simulate the negative Poison's ratio behavior of the plied yarn structure by keeping the modulus of the soft yarn unchanged. The simulation results with different values of E^* for a tensile strain of 0.03 are shown in Fig. 7. It can be seen that the negative Poisson's ratio effect of the auxetic plied yarn is increased with increasing E^*. Hence, selecting a stiff yarn with a high modulus is an effective way to obtain an auxetic plied yarn with a significant negative Poisson's ratio effect.

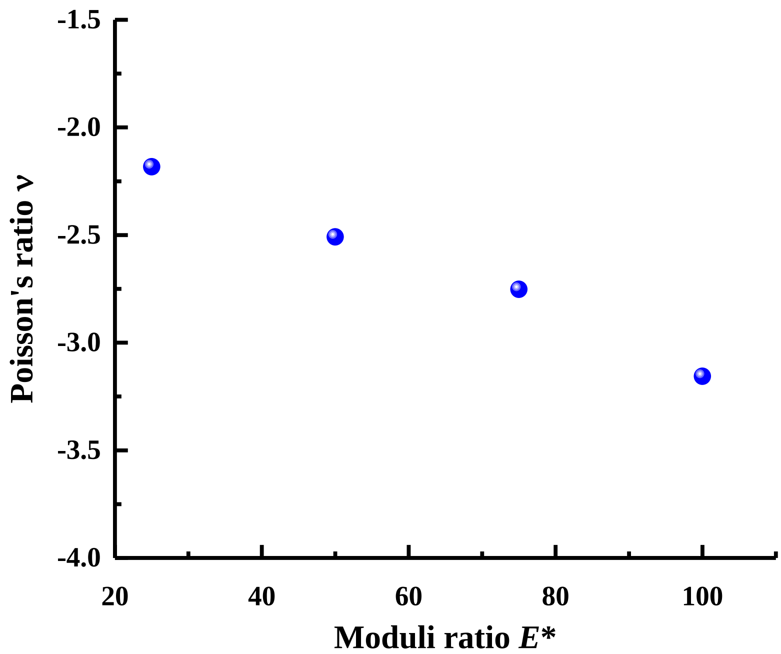

Figure 7. Poisson's ratio as a function of moduli ratio E^* for a given tensile strain of 0.03

5. Conclusions

The finite element models with different material properties and tilt angles of the stiff yarn at the initial state were created and used to simulate the negative Poisson's ratio behavior of the auxetic plied yarn structure. The simulation results were compared with the experimental and geometrical analyses. The effects of yarn material properties including the modulus and friction were discussed. Based on the simulation results, the following conclusions can be drawn to guide the design and fabrication of the auxetic plied yarns.

1) The deformation behavior of the auxetic plied yarn structure in the initial stage of the extension process is significant affected by the tilt of the stiff yarn at the initial state. To obtain a more uniform, the more stable plied yarn structure should be produced to avoid the de-twisting trend of the stiff yarns at the initial state.

2) The friction between the component yarns can reduce the negative Poisson's ratio effect of the auxetic plied yarn structure. To produce a plied yarn with more significant negative Poisson's ratio effect, smoother component yarns with reduced friction coefficient should be used.

3) The moduli of component yarns have a significant effect on the negative Poisson's ratio effect of the auxetic plied yarn structure. To produce a plied yarn with more significant negative Poisson's ratio effect, stiff yarn with high modulus should be used.

Acknowledgment

This work was supported by the Research Grants Council of Hong Kong Special Administrative Region Government in the form of a GRF project [grant number 515713].

Declaration of conflicting interests

The authors declare that they have no conflict of interest.

References

1. **Evans KE and Alderson A. Auxetic materials: Functional materials and structures from lateral thinking! *Adv Mater* 2000; 12: 617-+. Review. DOI: 10.1002/(sici)1521-4095(200005)12:9<617::aid-adma617>3.0.co;2-3.**

2. Li S, Hassanin H, Attallah MM, et al. The development of TiNi-based negative Poisson's ratio structure using selective laser melting. *Acta Mater* 2016; 105: 75-83. Article. DOI: 10.1016/j.actamat.2015.12.017.

3. Bhullar SK. Three decades of auxetic polymers: a review. *e-Polymers* 2015; 15: 205-215. Review. DOI: 10.1515/epoly-2014-0193.

4. Lakes R. FOAM STRUCTURES WITH A NEGATIVE POISSONS RATIO. *Science* 1987; 235: 1038-1040. Article. DOI: 10.1126/science.235.4792.1038.

5. Liu YP and Hu H. A review on auxetic structures and polymeric materials. *Sci Res Essays* 2010; 5: 1052-1063. Review.

6. Hu H, Wang ZY and Liu S. Development of auxetic fabrics using flat knitting technology. *Text Res J* 2011; 81: 1493-1502. Article. DOI: 10.1177/0040517511404594.

7. Zhou L, Zeng JF, Jiang LL, et al. Low-velocity impact properties of 3D auxetic textile composite. *J Mater Sci* 2018; 53: 3899-3914. Article. DOI: 10.1007/s10853-017-1789-8.

8. Ma PB, Chang YP, Boakye A, et al. Review on the knitted structures with auxetic effect. *J Text Inst* 2017; 108: 947-961. Review. DOI: 10.1080/00405000.2016.1204901.

9. Hu JY, Zhou Y, Liu ZS, et al. Pattern Switching in Soft Cellular Structures and Hydrogel-Elastomer Composite Materials under Compression. *Polymers* 2017; 9: 13. Article. DOI: 22910.3390/polym9060229.

10. Alderson A and Alderson KL. Auxetic materials. *Proc Inst Mech Eng Part G-J Aerosp Eng* 2007; 221: 565-575. Article. DOI: 10.1243/09544100jaero185.

11. Alderson KL and Evans KE. THE FABRICATION OF MICROPOROUS POLYETHYLENE HAVING A NEGATIVE POISSON RATIO. *Polymer* 1992; 33: 4435-4438. Article. DOI: 10.1016/0032-3861(92)90294-7.

12. Ge ZY, Hu H and Liu SR. A novel plied yarn structure with negative Poisson's ratio. *J Text Inst* 2016; 107: 578-588. Article. DOI: 10.1080/00405000.2015.1049069.

13. Zeng JF, Hu H and Zhou L. A study on negative Poisson's ratio effect of 3D auxetic orthogonal textile composites under compression. *Smart Mater Struct* 2017; 26: 14. Article. DOI: 06501410.1088/1361-665X/aa6fe6.

14. Fu MH, Chen Y and Hu LL. Bilinear elastic characteristic of enhanced auxetic honeycombs. *Compos Struct* 2017; 175: 101-110. Article. DOI: 10.1016/j.compstruct.2017.04.007.

15. Evans KE, Nkansah MA and Hutchinson IJ. MODELING NEGATIVE POISSON RATIO EFFECTS IN NETWORK-EMBEDDED COMPOSITES. *Acta Metall Mater* 1992; 40: 2463-2469. Article. DOI: 10.1016/0956-7151(92)90164-a.

16. Ge ZY, Hu H and Liu YP. Numerical analysis of deformation behavior of a 3D textile structure with negative Poisson's ratio under compression. *Textile Research Journal* 2015; 85: 548-557. Article. DOI: 10.1177/0040517514548813.

17. Wang ZY and Hu H. Auxetic materials and their potential applications in textiles. *Text Res J* 2014; 84: 1600-1611. Article. DOI: 10.1177/0040517512449051.

18. Critchley R, Corni I, Wharton JA, et al. A review of the manufacture, mechanical properties and potential applications of auxetic foams. *Phys Status Solidi B-Basic Solid State Phys* 2013; 250: 1963-1982. Article. DOI: 10.1002/pssb.201248550.

19. Allen T, Hewage T, Newton-Mann C, et al. Fabrication of Auxetic Foam Sheets for Sports Applications. *Physica Status Solidi B-Basic Solid State Physics* 2017; 254: 1700596. Article. DOI: 170059610.1002/pssb.201700596.

20. Lim T-C. *Auxetic Materials and Structures*. Springer, 2015.

21. Mir M, Ali MN, Sami J, et al. Review of Mechanics and Applications of Auxetic Structures. *Adv Mater Sci Eng* 2014: 17. Review. DOI: 75349610.1155/2014/753496.

22. Lakes RS. Negative-Poisson's-Ratio Materials: Auxetic Solids. In: Clarke DR (ed) *Annual Review of Materials Research, Vol 47*. Palo Alto: Annual Reviews, 2017, pp.63-81.

23. McAfee J and Faisal NH. Parametric sensitivity analysis to maximise auxetic effect of polymeric fibre based helical yarn. *Composite Structures* 2017; 162: 1-12. DOI: https://doi.org/10.1016/j.compstruct.2016.11.077.

24. Zhang GH, Ghita O and Evans KE. The fabrication and mechanical properties of a novel 3-component auxetic structure for composites. *Composites Science and Technology* 2015; 117: 257-267. DOI: 10.1016/j.compscitech.2015.06.012.

25. Du ZQ, Zhou M, He LG, et al. Study on negative Poisson's ratio of auxetic yarn under tension: Part 2-Experimental verification. *Textile Research Journal* 2015; 85: 768-774. DOI: 10.1177/0040517514549987.

26. Du ZQ, Zhou M, Liu HL, et al. Study on negative Poisson's ratio of auxetic yarn under tension: Part 1-Theoretical analysis. *Textile Research Journal* 2015; 85: 487-498. DOI: 10.1177/0040517514549985.

27. Bhattacharya S, Zhang GH, Ghita O, et al. The variation in Poisson's ratio caused by interactions between core and wrap in helical composite auxetic yarns. *Composites Science and Technology* 2014; 102: 87-93. DOI: 10.1016/j.compscitech.2014.07.023.

28. Lim TC. Semi-auxetic yarns. *Physica Status Solidi B-Basic Solid State Physics* 2014; 251: 273-280. DOI: 10.1002/pssb.201384237.

29. Sloan MR, Wright JR and Evans KE. The helical auxetic yarn - A novel structure for composites and textiles; geometry, manufacture and mechanical properties. *Mechanics of Materials* 2011; 43: 476-486. DOI: 10.1016/j.mechmat.2011.05.003.

30. Wright JR, Sloan MR and Evans KE. Tensile properties of helical auxetic structures: A numerical study. *Journal of Applied Physics* 2010; 108: 044905. DOI: 04490510.1063/1.3465378.

31. Ng WS and Hu H. Tensile and Deformation Behavior of Auxetic Plied Yarns. *Physica Status Solidi B-Basic Solid State Physics* 2017; 254: 1600790. Article. DOI: 160079010.1002/pssb.201600790.

32. Zeng J and Hu H. A theoretical analysis of deformation behavior of auxetic plied yarn structure. *Smart Materials and Structures* 2018; 27: 075003.